# ACHIEVED PERFORMANCE OF AN ALL X-BAND PHOTO-INJECTOR∗

C. Limborg-Deprey, C. Adolphsen, D. McCormick, M. Dunning, K. Jobe, H. Li, T. Raubenheimer,
A. Vrielink, T. Vecchione, F. Wang and S. Weathersby, SLAC National Accelerator Laboratory,
Menlo Park, CA, 94025, USA

## Abstract

Building more compact accelerators to deliver high brightness electron beams for the generation of high flux, highly coherent radiation is a priority for the photon science community. A relatively straightforward reduction in footprint can be achieved by using high-gradient X-Band (11.4 GHz) RF technology. To this end, an X-Band injector consisting of a 5.5 cell RF gun and a 1-m long linac has been commissioned at SLAC. It delivers an 85 MeV electron beam with peak brightness somewhat better than that achieved in S-Band photoinjectors, such as the one developed for the Linac Coherent Light Source (LCLS). The X-band RF gun operates with up to a 200 MV/m peak field on the cathode, and has been used to produce bunches of a few pC to 1.2 nC in charge. Notably, bunch lengths as short as 120 fs rms have been measured for charges of 5 pC ($\sim 3\times10^7$ electrons), and normalized transverse emittances as small as 0.22 mm-mrad have been measured for this same charge level. Bunch lengths as short as 400 (250) fs rms have been achieved for electron bunches of 100 (20) pC with transverse normalized emittances of 0.7 (0.35) mm-mrad. We report on the performance and the lessons learned from the operation and optimization of this first generation X-Band gun.

## INTRODUCTION

There has long been an interest in having compact electron sources for a variety of accelerator applications such as FELs, electron scattering experiments, imaging and radiation therapy. In particular, large-scale X-ray Free Electron Lasers (XFELs), which are the ultimate tunable microscopes to probe matter on the atomic scale, have drive linacs that range from a few hundreds of meters to about one kilometer in length. Currently, they are based on three RF technologies: 1.3 GHz, 24 MV/m, superconducting L-Band [1], 2.86 GHz, 17 MV/m, room-temperature S-Band [2,3], and 5.7 GHz, 35 MV/m, room temperature C-Band at SACLA [4] and SwissFEL[5].

For the future, there is interest in reducing the linac length to the 100-m level [6], by using room temperature, high gradient (70-100 MV/m), 11.4 GHz X-Band technology that was developed for the NLC/GLC programs in the 1990's and early 2000's while still delivering the high brightness electrons needed to produce high peak intensity photon bunches. Other promising very-high gradient (1-10 GV/m) accelerator technologies – laser generated plasma wakefield acceleration [7] and beam generated plasma acceleration [8] - are being developed although the beam quality, reproducibility and stability are still far from that needed to drive FELs.

As an offshoot of the ∼ 100 M$ X-band program at SLAC, an X-Band gun was built in the mid-2000's for a compact Compton source that was to be used for a medical application [9]. This was done during a period when the LCLS S-band gun was being developed and there was much interest in photoinjectors. This first X-band gun operated with up to a 200 MV/m cathode peak field, but a detailed beam characterization was never performed as the program ended early.

In the late 2000's, there was renewed interest in X-band technology from the experience with the X-band harmonic linearizer used at LCLS and other FELS, the desire by laboratories to fit next generation light sources into existing lab space [8] and applications for compact gamma-ray Compton sources [9]. However, unlike S-band and C-band technology at that time, commercial high power klystrons were not available (one company makes them today), and a low-emittance X-band demonstration linac did not exist. To address this second issue, that is, showing that high gradient acceleration and low emittance bunches are simultaneously achievable, an all X-band injector was built in the Next Linear Collider Test Area (NLCTA) at SLAC. Called the X-Band Test Area (XTA), this accelerator runs parallel to the original beamline at the downstream end of the accelerator enclosure, but it is only about 7 m long.

## THE X-BAND TEST AREA

### RF Gun

The RF gun presently in operation at XTA is denoted "Mark-0," and is essentially a copy of the 5.5 cell original design (using leftover parts). The idea was to use this gun to debug the XTA before a new, more optimized design, call the Mark-1 was deployed. The new gun design was developed in collaboration with LLNL, and has 5.6 cells, a race-rack coupler, elliptical contoured irises, an RF coupling that better balances pulsed heating with cavity fill time and a larger mode separation [10]. Two Mark-1 guns were built, one that was to be used in XTA (but now would require additional funding to test), and one that was installed at LLNL in 2014[10]. The Mark-1 gun has recently been commissioned and its performance is reported in [11]. In this paper and [12], we present the performance of the Mark-0 gun at XTA.

The RF, thermal and mechanical designs have been described in [11]. Note that the cathode is brazed to the first cell, which is half as long as the standard cells in the

Mark-0 gun. The cathode is consequently non-demountable. The copper cathode diameter is as large as the cell internal diameter of 21.8 mm. However the irises separating the cells limit the aperture along the gun to 8 mm, and the cathode region accessible by the laser is limited to a disk of approximately 7 mm.

### The XTA Beamline and Power Distribution

A photo of the XTA is shown in Fig. 1. To power the XTA, a single RF source, an XL4 klystron, is utilized to deliver power both to the RF gun, where the electrons are generated and first accelerated, and to the single accelerator structure. The klystron provides up to 50 MW of X-band RF power in a 1.5 μs long pulse, which is compressed in 40 m long SLED-II lines [13] up to 200 MW in a 250 ns long pulse. The maximum klystron repetition rate is 60 Hz, although we generally ran at 10 Hz to limit beam-induced radiation.
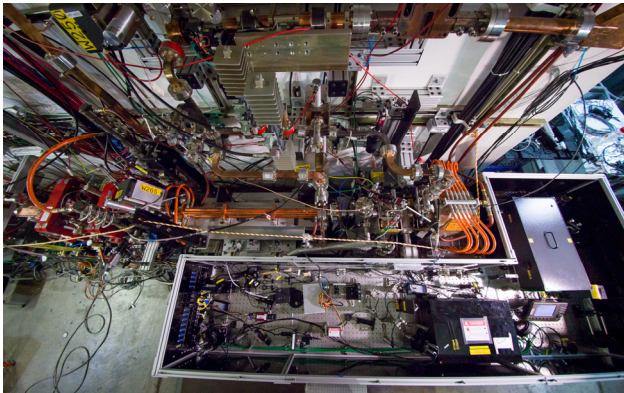


Figure 1: X-Band Test Area beamline. The 1.05 m long copper accelerator structure is seen in the middle of the photo, and one of three phase shifters is visible on the wall at the top of the picture.

The power distribution is schematically shown in Fig. 2. To produce a peak field of 200 M/m on the cathode with a 180 ns square input pulse, 17 MW is required at the input to the gun. We tune the gun line phase shifters to achieve the desired cathode field with typically 140 MW to 180 MW of SLED-II output power, out of which 75 MW to 97 MW powers the 1.05 m long, 'T105' accelerator structure for the subsequent bunch acceleration. Generation and acceleration of photoelectron bunches up to 85 MeV have been demonstrated in the gun plus accelerator section, which is only 1.8 m long. Inferring the cathode gradient based on the SLED-II power has much uncertainty due to unknown RF mismatches in the waveguides runs, setting accuracy of the gun phase shifters and non-ideal RF pulse shapes. As discussed in the measurement section, comparing laser-to-beam relative-time-of-arrival (RTOA) measurements to predictions is probably the best calibration of the cathode field in the gun for the high gradient field and indicates that a 150 MW SLED-II pulse produces a 190 MV/m cathode field.
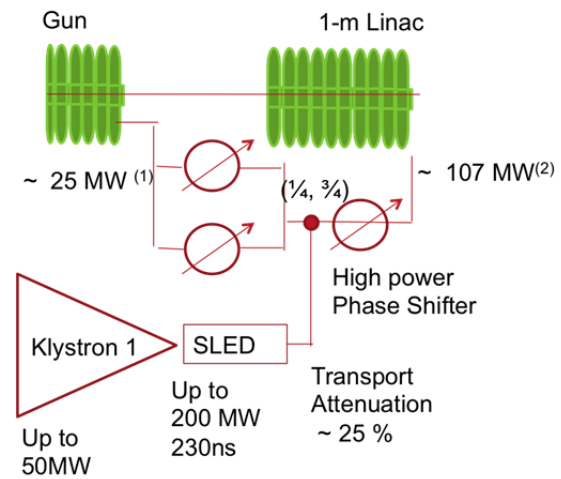
Figure 2: Schematic of the XTA power distribution.

## BEAM DYNAMICS IN THE GUN

### Advantages of a High Cathode Field Gradient

In Fig. 3, the increase in the energy of an electron in a gun (expressed by γ) is shown during the first 33 ps of acceleration, during which the electrons travel several mm beyond the cathode. For this calculation, the S-Band gun is assumed to operate with a 120 MV/m cathode field and the X-Band gun with a 200 MV/m field, which are near the upper limits for reliable operation at these two frequencies (at these field levels, breakdown events occur rarely). As described in [14] the transverse space charge force has a $1/\gamma^2$ dependence and the primary detrimental space charge effect occurs in the region where γ is less than about two. As seen in Fig. 3, γ reaches this level roughly twice as fast in the X-band case.
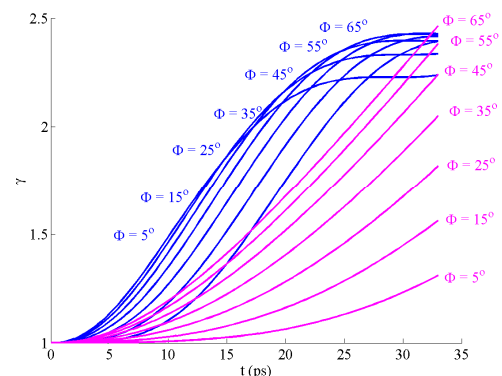


Figure 3: Evolution of γ with time for a single electron in a 200 MV/m X-Band gun (blue) and a 120 MV/m S-Band gun (magenta) for different initial RF phases.

Due to the rapid increase in γ, the bunch length is frozen 1- 3 mm downstream of the cathode, approximately 1 mm for low space charge and 3 mm for high space charge. Smaller transverse emittances are achieved with higher gradient fields in the RF gun. The high field present in the X-Band gun also allows operation at higher charges for smaller laser spot sizes. The space charge

limit equation, which is the direct consequence of Gauss's law, is given in Equation 1, where E is the cathode field, Q the charge and r the laser spot radius. Equation 1 is valid as long as the aspect ratio of the laser pulse is similar to that of a "pancake". For a time-elongated laser profile, i.e., "cigar shape", the space charge limit can be violated [15,16] and the charge proportional to the 3/2 power of the product of radius times acceleration field.

$$E = \frac{\sigma}{\varepsilon_o} = \frac{Q}{\varepsilon_o\,\pi r^2} \qquad (1)$$

Note that the thermal emittance is also expected to increase in the presence of high gradient fields [17,18]. The magnitude increase in thermal emittance is however very dependent on the quality and history of the cathode. A detailed comparison of beam dynamics in the 5.5 X-Band gun and in the 1.5 cell S-Band gun, referred to as the "LCLS gun", has been given in [12] for low, moderate and high space charge effects. Fig. 4 summarizes the optimum emittance, bunch length and brightness for both an X-Band gun and an S-Band gun operated with fields of 200 MV/m and 120 MV/m on the cathode respectively.
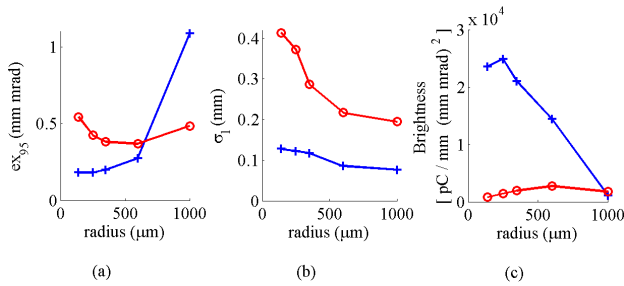


Figure 4: Results from 100 pC bunch charge parameter scans as a function of the laser spot size radius where the blue crosses are for X-band (200 MV/m cathode field) and the red circles are for S-band (120 MV/m cathode field: (a) minimum 95% transverse emittance, (b) minimum bunch length and (c) maximum peak brightness.

## X-BAND GUN IN OPERATION

### Dark Current from the RF Gun

The term "dark current" refers to the net electron charge from field emission that is captured and accelerated during a pulse. It had been generally believed that a high gradient RF gun would be of limited use due to high levels of dark currents that would be co-accelerated. The Mark-0 gun produces dark currents at the level of hundreds of pC, as shown in Fig. 5, but we can still achieve low emittance, low charge (a few pC) electron bunches. For our nominal operating conditions, the dark current is typically limited to 10 pC after acceleration in the linac where the 6 mm diameter beam tubes at each end of the 1 m long accelerator structure act as collimators. The transmitted dark current has a wide energy spread and transverse size, and thus can be further collimated if necessary.
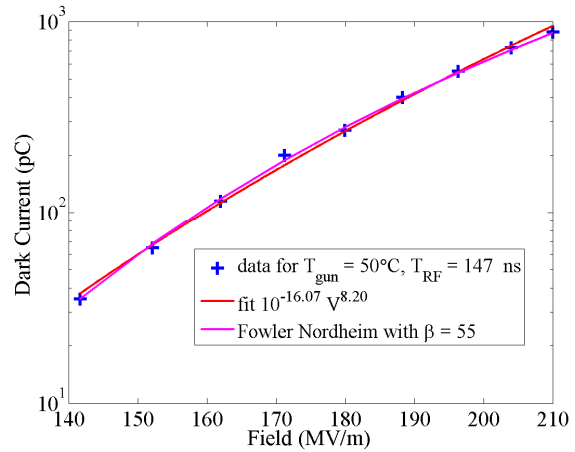


Figure 5: Integrated dark current as a function of cathode gradient with 147 ns long RF pulses measured 0.56 m from the cathode.

The gun dark current originates primarily from the cathode and is believed to be enhanced by the surface roughness as visible in Fig. 6a. A zoomed image of the illuminated cathode, Fig. 6b shows strong variations in the surface topology at a scale of typically 100 μm, but also down to 20 μm or less.
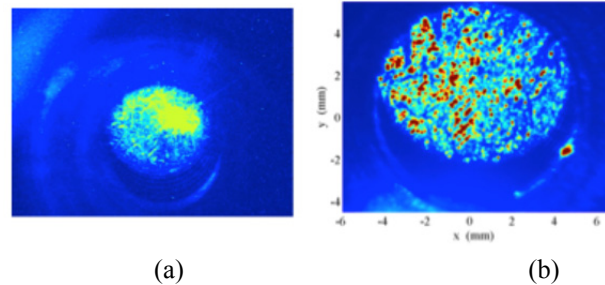


Figure 6: Cathode surface images taken through the extraction mirror (opposite to the injection mirror) using a camera just outside of the vacuum chamber. (a) This image was taken using visible light after the gun was RF conditioned but before the first photoelectron beam was generated. The surface already appears damaged at this stage. (b) Cathode surface imaged with visible light after 2 years of operation of the gun. The center circle of bright spots fills the entire 7 mm diameter cathode.

### Measurement of Beam Energy

The electron beam energy at the gun exit was measured by deflecting the beam with a corrector magnet and by measuring the downstream change in position. We did this using both horizontal and vertical corrector magnets located 20 cm upstream of a YAG profile monitor, and the results are shown in Fig. 7. The energies inferred from the horizontal and vertical kicks agree well. The highest gradients could not be verified with this method as the dark current hitting the screen obscured the photoelectron beam.
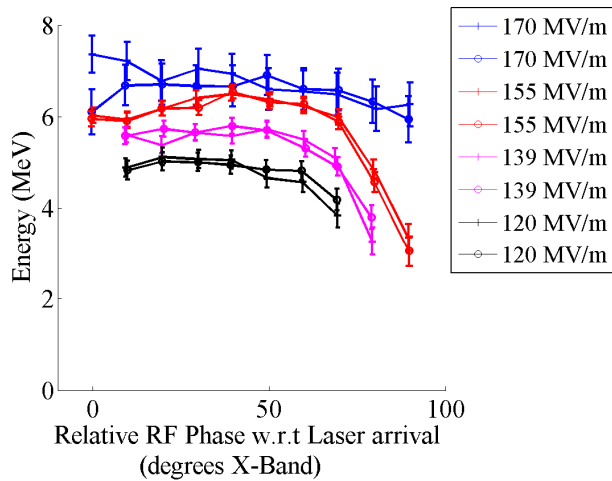
Figure 7: Bunch energy versus RF-to-laser phase measured after the gun at different cathode gradients using either the horizontal (data points with crosses) or vertical corrector magnets (data points with circles).

The relative time of arrival (RTOA) of the electron bunch with respect to the RF phase was measured using the phase of the signal from an X-Band single-cell cavity located just upstream of the linac. Measurements were performed for a large range of power levels and presented in Fig. 8. The single cell resonant frequency was chosen to be 12.85 GHz to suppress the dark current signal at 11.424 GHz. The 150 MW data could be fitted with a gun field of 190 MV/m as shown in Fig. 9. Note that the gun was operated up to 215 MV/m with a SLED-II power output of 190 MW. The data presented in Fig. 9 is narrowed to a phase range where the time-of-flight is minimally dependent on the initial phase and thus the timing jitter minimum. The rms arrival time jitter is as small as 0.5 deg. X-Band (ie 125 fs). The dominant contribution comes from the laser pulse timing jitter.
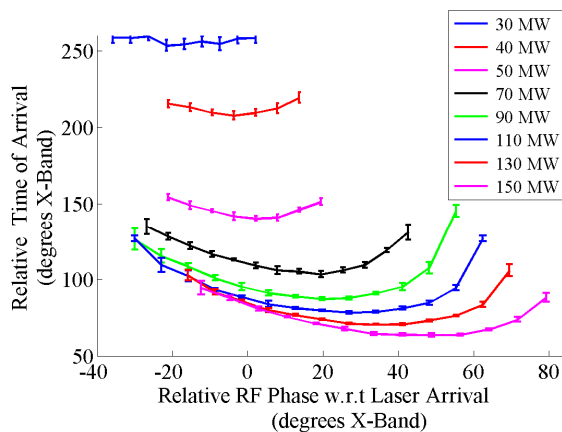


Figure 8: Measured Relative Time of Arrival (converted to phase at 11.424 GHz) versus RF phase relative to the laser arrival for different SLED-II power levels. The RF pulse length was 140 ns.
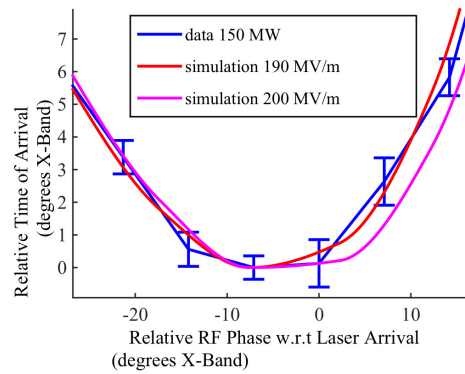


Figure 9: Zoom-in of the data near the RTOA minimum. RMS fluctuations were calculated using 50 sample points.

## Measurement of Bunch Length

The bunch lengths were measured using a transverse X-Band deflector powered by an independent klystron. The details of the measurements are described in [12]. The black-cross data points of Fig. 10 were measured for an electron beam generated using a 60 fs FWHM laser pulse and a 1 mm spot radius. The curves in the plot are simulations assuming the same laser duration, spot radii of 0.5 mm and 1 mm, a gun solenoid field of 5.7 kG and a cathode field of 200 MV/m. The agreement is fairly good.

The best result was 270 A with 290 pC in a 460 fs long bunch (one of the black data points) and could be reproduced on several occasions once the linac was tuned and reasonable stability was achieved. Higher peak currents are expected for higher bunch charges. A data point in Fig. 10 of particular interest for applications requiring short bunches is the one with 5 pC charge ($3 \times 10^7$ electrons) where a 125 fs rms long bunch was measured and was quite reproducible.
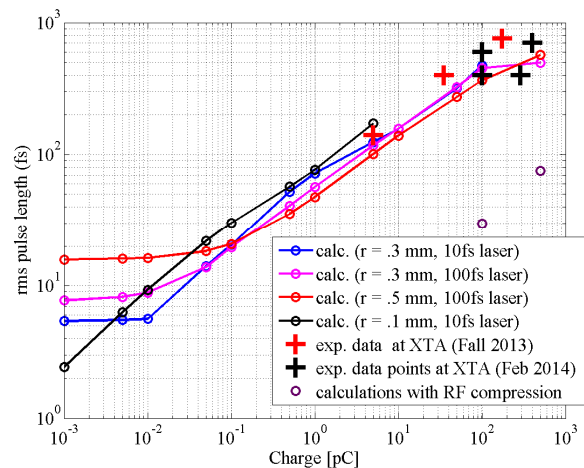


Figure 10: Bunch lengths measured with a transverse deflector versus bunch charge, and simulated data. Circles are simulation data and crosses experimental data.

### Transverse Emittance Measurements

Transverse emittances were calculated from quadrupole scans by measuring the beam size of visible light profiles generated by the beam hitting Optical Transition Radiation (OTR) screens. The imaging system had a resolution of 15 μm. Emittances were typically optimized and measured at beam energies around 70 MeV. For this energy and the bunch sizes measured, the space charge effects were negligible. The optimization procedure to reach the minimum emittance consisted of steering the laser to position it at the cathode center, or to a "sweet spot", then steering the beam through the linac and minimizing the bunch energy spread. The emittance was then measured for various solenoid values and RF-to-laser phases. The laser pulses were as short as 50 fs FWHM. The best emittance values measured after optimization and resolution corrections were 0.22 mm-mrad at 5 pC, 0.43 mm-mrad at 30 pC and 0.66 mm-mrad at 100pC. All these values were reproducible but unfortunately they were obtained after the gun had already been damaged.

Table 1: Margin Specifications

| Q(pC) | 5 | 10 | 30 | 100 |
|---|---|---|---|---|
| ε (mm-mrad) | 0.22 | 0.32/0.28 | 0.47/0.43 | 0.7 |

The gun cathode was damaged from repetitive breakdowns during the initial RF conditioning as visible in Fig. 6a. The strikes of the high peak power laser pulses also contributed to damage the cathode. It was not possible to measure good emittances for spot sizes larger than 1 mm. However, for chosen areas, the thermal emittance could be verified to be in the range of 1 mm-mrad per mm rms.

### Stability

The transverse stability was typically between 5 and 10 μm rms. For the typical 40 μm rms beam sizes, this corresponds to 12 to 25% of the beam size. The transverse jitter is a consequence of energy fluctuations at the gun exit. This principally comes from the power supply fluctuations of the modulator high voltage. Simulations are reported in [12] exhibiting how a beam offset by 300 μm on the cathode can move by 20 μm at the end of the beamline if the energy jitter is in the $10^{-3}$ range.
Our modulator voltage typically has 175 ppm fluctuations. This translates into $3.10^{-4}$ fluctuations in field amplitude. Combined with LLRF jitter, and laser jitter, the typical energy fluctuation at the spectrometer at the end of the beamline was in the $5.10^{-4}$ range.

## CONCLUSIONS

An 85MeV, 2-m long e-beam all X-Band photo-injector was built and commissioned. Good beam quality was obtained with a brightness slightly exceeding that out of the LCLS S-Band injector despite a damaged cathode. For the next generation of X-Band guns to be fabricated, we highly recommend building a gun with a demountable cathode. We recommend a design of a 3.5 cell gun instead of 5.5 cells which calls for a solenoid with reduced strength and a better clearance for the laser injection. We recommend following a very slow RF processing procedure, including backing off dramatically the power level after a single RF breakdown. For applications requiring challenging transverse stability, ie at the μm level, and energy stability at $10^{-4}$ or less, a low noise modulator with performances at least as good as 50 ppm is needed.

## REFERENCES

[1] Altarelli.M, "XFEL: The European X-Ray Free-Electron Laser," Technical Design Report. Preprint DESY 2006-097, Preprint DESY, 2006-097.

[2] Emma.P, "First lasing and operation of an ångstrom-wavelength free-electron laser," *Nature Photon* , pp. 4, 641–647, 2010.

[3] Hwang.I, "FEL simulation of the 0.1-nm Hard X-ray from the PAL-XFEL," *J. Korean Physical Society,* pp. pp 212-213, January 2014, Volume 64, Issue 2 2014.

[4] Tanaka.T, "SCSS XFEL CDR," Riken Harima Institute, 2005.

[5] "SwissFEL CDR," April 2012.

[6] Y. Sun, et al "X-band rf driven FEL driver with optics linearization", PRST-AB 17, 10703 (2014).

[7] W. Leemans, et al. Multi-GeV Electron Beams from Capillary-Discharge-Guided Subpetawatt Laser Pulses in the Self- Trapping Regime, PRL 113, 245002 (2014).

[8] M. Litos, High-efficiency acceleration of an electron beam in a plasma wakefield accelerator, Nature (London) 515, 92 (2014).

[9] A. E. Vlieks, Recent measurements and plans for the SLAC Compton X-ray source, AIP Conf. Proc. 807, 481 (2006).

[10] Gibson.D.J, "Multi-GHz Pulse-Train X-Band Capability for Laser Compton X-Ray and Gamma-Ray Sources," *IPAC 2015*, Richmond, Virginia, USA, 2015.

[11] R. Marsh, "Modeling and design of an X-band rf photo-injector," PRST-AB 15, 102001 (2012).

[12] C.Limborg et al. "Performance of a first generation X-Band gun" , PR-AB, Vol 19, 053401, (2016).

[13] C.Nantista, "High Power RF Pulse Compression with SLED II at SLAC," *SLAC-PUB 6145,* 1993.

[14] K.Kim, RF and space charge effects in laser driven rf electron guns, NIM PR Sect. A 1045 275, 201 (1989).

[15] D. Filipetto, "Maximum current density and beam brightness achievable by laser-driven electron sources", 1047 Phys. Rev. ST Accel. Beams 17, 024201 (2014).

[16] R. Li, Nanometer emittance ultralow charge beams from rf photoinjectors, PRST-AB 15, 090702 (2012).

[17] C. P. Hauri, Intrinsic Emittance Reduction of an Electron Beam from Metal Photocathodes, PRL 104, 234802 (2010).

[18] D. Dowell and J. Schmerge, Quantum efficiency and thermal emittance of metal photocathodes, PRST-AB 12, 1 119901 (2009).